Analysis of Rectilinear Rivulet Flow

A liquid flowing over a nonwettable surface can form rivulets of various types. The regime of rectilinear rivulet flow plays a key role in that it provides the basis for the study of the other regimes.

An analytical solution for the velocity distribution of rectilinear rivulet flow down a vertical plate is derived. A generalized Ritz-Galerkin method is used to obtain a polynomial solution for the case of an inclined plate.

These results, unlike those of previous authors, enable one to calculate all the rectilinear flow properties of rivulets over the complete range of practical interest.

MICHAEL BENTWICH
DAVID GLASSER
JOCHEN KERN
DONALD WILLIAMS

Department of Chemical Engineering
University of the Witwatersrand
Johannesburg 2001, South Africa

SCOPE

The flow of rivulets down inclined surfaces occurs in many types of process equipment such as condensers, packed beds, and trickle flow reactors. A prerequisite for describing these processes scientifically is a knowledge of the velocity distribution within the rivulet. The velocity distribution in a laminar rivulet is of particular importance because it provides the basis for the understanding of other types of rivulet flow. Instabilities in the laminar rivulet are responsible for the transition to drop, meandering, and turbulent flow, for instance. A theoretical study of each of these phenomena would first require the solution to the laminar flow problem.

Previous methods have been limited to perturbation expansions for low contact angles or direct numerical analyses for flow down a vertical plate. The results are of limited use for the needs expressed above.

By means of a bipolar conformal transformation, an analytical solution is derived for the case of the vertical plate.

For the nonvertical case, the normalized velocity distribution (W) can be expressed in terms of two parameters which represent ratios of the forces acting, namely, the contact angle (θ) and the rivulet height made dimensionless with the capillary constant (Δ), and all cases are covered by the range $0 \leq \theta \leq 180$ deg., $0 \leq \Delta \leq 2 \sin(\theta/2)$.

CONCLUSIONS AND SIGNIFICANCE

The analytical solution for the vertical plate has the form of an infinite integral which was evaluated by using a thirty-two point Gaussian-Laguerre quadrature. This was also reduced to a series solution by the method of residues. The integral solution was used as a test for the Ritz-Galerkin method. It was found that up to contact angles of 140 deg. a four-term expansion produced adequate velocity profiles. Furthermore, with additional terms in the series, even better approximations are possible, although at contact angles above 150 deg. the number of terms required becomes excessive.

The same method was then employed to solve for the inclined flow problem. The above conclusion concerning the number of terms was found to hold with at least the same degree of accuracy; that is, four terms in the expansion gave adequate results up to 140 deg.

Under these circumstances, the results can be presented in graphs showing the mean velocity and the values of the four coefficients (A_{01}, A_{02}, A_{11}, A_{12}) over the range $0 \leq \theta \leq 140$ deg.

All the useful results produced in this paper are summarized graphically. In conjunction with the interface equations, they provide a complete and compact description of the velocity profiles in a laminar flow rivulet over the entire range of practical interest.

The generality and simplicity of the results is such that they can be readily used for the analysis of transfer processes as well as stability problems.

A large number of transfer operations involve the simultaneous presence of gas, liquid, and solid phases. Evaporation, condensation, and packed-bed processes are a few examples. It is frequently assumed, and often found, that the liquid flows as a film over the solid surface. However, depending on the dynamic conditions as well as on the interfacial tensions, such a film can break up into rivulets which may be desirable, as in the case of the trickle-bed reactor, or undesirable, as in a thin film evaporator. In any event, the changed hydrodynamic characteristics will have a marked effect on the heat or mass transfer in such a system.

When looking at a surface over which rivulets are flowing, one observes a rather chaotic picture with the surface covered by different types of rivulets. In a recent classification, Kern (1975) has shown that most types of rivulets can be described with reference to straight laminar flow. It is the aim of this article to provide the hydrodynamic relationships describing the velocity distribution in a single laminar rivulet. On the basis of these results, one is then able to investigate discharge, heat, and mass transfer as well as stability.

Two difficulties are encountered in attempting an analytic solution to this problem. They are both related to the gas-liquid interface which forms part of the boundary of the flow cross section. First, in the general case, this interface cannot be specified in explicit form; it is the well-known elastica which, only for a vanishing gravity component, reduces to the arc of a circle. (This latter case of a rivulet flowing in the direction of gravity is of particu-

M. Bentwich is on leave from the Department of Fluid Mechanics and Heat Transfer, University of Tel Aviv, Ramat Aviv, Israel.

lar interest since it can be solved analytically.) The second problem arises from the fact that the boundary conditions are of a mixed type, and this further complicates the solution of the governing equations.

All previous approaches were limited in that they either considered a drastically simplified problem for analytic treatment or proceeded to a direct numerical simulation. The latter approach results in a set of numbers which are often inconvenient for further studies. Towell and Rothfeld (1966) limited their analysis to very flat rivulets and contact angles less than 20 deg. In that case, experiment shows that a parabolic (one dimensional) velocity distribution is satisfactory. Kern (1969) presented a numerical finite-difference solution to the specific case of constant interfacial curvature. Good agreement with experimental results was found up to a contact angle of approximately 100 deg. Allen and Biggin (1974) improved the solution of Towell and Rothfeld by expanding the velocity as a power series and solving the first-order problem. For comparison, they present a set of isovelocity lines computed with a finite element scheme. Although the improvement in accuracy is difficult to assess from just one result, it appears that the first-order solution becomes quite inaccurate for large interfacial curvatures which are encountered with contact angles above 50 deg. The present approach eliminates these shortcomings and yields accurate results for any contact angle of practical interest, that is, up to values of 150 deg.

We first present an analytic solution to the vertical flow problem against which our series solution can be checked. The series solution is then obtained for the general case of flow over an inclined surface.

VERTICAL FLOW

In the following it is assumed that flow is parallel to the gravity vector so that the flow cross section of the rivulet is just the segment of a circle (Figure 1). The following assumptions are made: steady and laminar flow over a flat and vertical plate, one-dimensional flow parallel to the z axis, incompressible Newtonian fluid, no slip at the solid-liquid interface, and no shear at the liquid-gas interface. Under these conditions, the Navier-Stokes equations reduce to

$$\frac{\partial P}{\partial x} = 0 \tag{1}$$

$$\frac{\partial P}{\partial y} = 0 \tag{2}$$

$$\frac{\partial^2 w}{\partial x^2} + \frac{\partial^2 w}{\partial y^2} = -g/\nu \tag{3}$$

The boundary conditions result from the fourth and fifth assumptions and are

$$w(|x| \leq R \sin\theta, y = 0) = 0 \tag{4}$$

and

$$\left.\begin{aligned} &\frac{\partial w}{\partial x}\, x + \frac{\partial w}{\partial y}\,(y + D) = 0 \\ \text{on}\quad &x^2 + (y + D)^2 = R^2 \end{aligned}\right\} \tag{5}$$

Equation (5) simply expresses, in Cartesian coordinates, the vanishing shear normal to the gas-liquid interface.

For direct comparison with the corresponding film analysis, the maximum rivulet height δ is introduced as a reference length. For vertical flow

$$\delta = R(1 - \cos\theta) \tag{6}$$

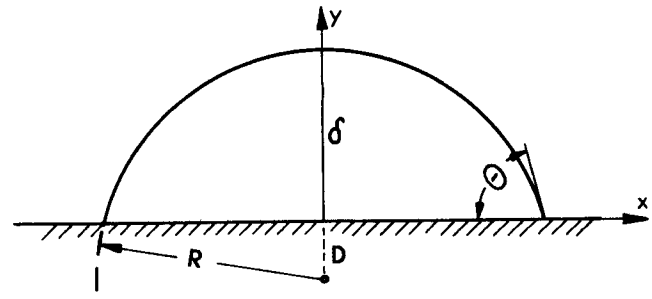

Fig. 1. Coordinate system for vertical rectilinear flow.

With

$$X = x/\delta, \quad Y = y/\delta, \quad \text{and} \quad W = \frac{w \cdot \nu}{g\delta^2} \tag{7}$$

the governing equation becomes

$$\frac{\partial^2 W}{\partial X^2} + \frac{\partial^2 W}{\partial Y^2} = -1 \tag{3a}$$

The transformed boundary conditions are

$$W(|X| \leq \alpha_s, \quad Y = 0) = 0 \tag{4a}$$

where

$$\alpha_s = \sin\theta/(1 - \cos\theta)$$

and

$$\left.\begin{aligned} &\frac{\partial W}{\partial X} X + \frac{\partial W}{\partial Y}(Y + \alpha_c) = 0 \\ \text{on}\quad &X^2 + (Y + \alpha_c)^2 = (\alpha_s + \alpha_c)^2 \end{aligned}\right\} \tag{5a}$$

where

$$\alpha_c = \cos\theta/(1 - \cos\theta)$$

Methods of Solution

An exact analytic solution to Equation (3a) subject to the boundary conditions (4a) and (5a) is obtained by conformal mapping. Formally, the solution can be expressed as

$$W = -\left(\frac{Y^2}{2} + \frac{Y}{2}\alpha_c\right) + \phi \tag{8}$$

where ϕ is a harmonic function. The expression in the bracket is one of many possible particular solutions. The choice made here simplifies the algebraic manipulations which are required to evaluate ϕ. Clearly, W is symmetric with respect to X, and in view of the form (8), so is ϕ. Also, it follows from condition (4a) that ϕ vanishes on

$$-\alpha_s < X < \alpha_s, \quad Y = 0$$

Admittedly, ϕ would have vanished on the solid boundary with any term linear in Y^n, n > 0. The choice $-\alpha_c Y/2$ simplifies the treatment of the condition imposed on the arc bounding the domain under discussion.

By choosing the appropriate logarithmic branch, the transformation

$$\zeta = \xi + i\eta = \ln\left[(z - \alpha_s)/(z + \alpha_s)\right] \tag{9}$$

maps the domain of flow onto the infinite strip ($\gamma < \eta < \pi$, $-\infty < \xi < \infty$). Here (ξ, η) are the so-called bipolar coordinates which have the following geometric significance (see Figure 2): η is the angle between the lines joining a generic point with the poles $(-\alpha_s, 0)$ and $(\alpha_s, 0)$, and ξ is the logarithm of the ratio of their respective lengths. As explained in a paper by Bentwich (1976) on two-phase Poiseulle flow, this transformation has three discernable features. First, it is conformal so that ϕ is harmonic not only in (X, Y) but also in (ξ, η). Second, the transformation maps the center line $X = 0$ onto $\xi = 0$. Therefore, the symmetry of ϕ with respect

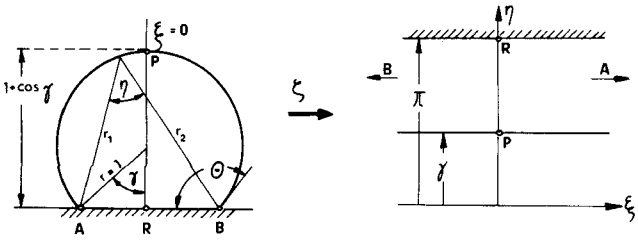

Fig. 2. Coordinate transformation for bipolar solution.

to X gives rise to symmetry with respect to ξ. Lastly, the chord and arc along which conditions (4*a*) and (5*a*) are imposed are conveniently defined by $\eta = \pi$ and $\eta = \gamma \equiv (\pi - \theta)$, respectively. Evidently the general expression for ϕ, which is harmonic, symmetric with respect to ξ, and vanishes on $\eta = \pi$, is given by the cosine integral in the following expression:

$$W = -\frac{Y^2}{2} - \alpha_c \frac{Y}{2} + (\alpha_s^2 + \alpha_c^2) \int_0^\infty f(\beta) \sinh[\beta(\pi - \eta)] \cos(\beta\xi) d\beta \tag{10}$$

In terms of the bipolar coordinates condition (5*a*) reduces to

$$\frac{1}{(\alpha_s^2 + \alpha_c^2)} \partial W/\partial\eta \Big|_\gamma = 0 = -\sin^3\gamma \frac{(\cos\gamma\cosh\xi - 1)}{(\cosh\xi - \cos\gamma)^3} - \frac{1}{2}\sin\gamma\cos\gamma \frac{(\cosh\xi\cos\gamma - 1)}{(\cosh\xi - \cos\gamma)^2} - \int_0^\infty f(\beta)\, \beta\cosh[\beta(\pi - \gamma)] \cos(\beta\xi) d\beta$$

where the first two terms are derived by differentiating Y^2 and Y with respect to η. $Y(\xi, \eta)$ is obtained from the transformation (9). Standard procedure is adopted to invert the cosine integral and hence solve for $f(\beta)$. The solution for W is thus found to be

$$W = -\frac{Y^2}{2} - \alpha_c \frac{Y}{2} + (\alpha_s^2 + \alpha_c^2) \int_0^\infty [1 + (\sin^2\gamma)\beta^2] \frac{1}{\beta} \frac{\sinh[\beta(\pi - \gamma)] \sinh[\beta(\pi - \eta)]}{\sinh(\beta\pi)\cosh[\beta(\pi - \gamma]} \times \cos(\beta\xi) d\beta \tag{11}$$

This form readily yields numerical results for the center line $\xi = 0$. In such cases, $\cos(\beta\xi)$ is unity, and for large β the integrand is very nearly

$$[\beta^{-1} + (\sin\gamma)^2 \beta] \exp(-\beta\gamma)$$

Thus, one can integrate analytically for the tail end of the integral over the range $\bar{\beta} < \beta < \infty$. Over the finite range $0 < \beta < \bar{\beta}$ one can substitute an approximate summation for the integral. The entire computation can be carried out on a pocket computer.

Away from the center line, the integration becomes difficult because of the repeated sign change of $\cos(\beta\xi)$. But in this case, the cosine integral over the semi-infinite range can be replaced by an integral over the entire β range with $1/2 \exp(i\beta\xi)$ replacing $\cos(\beta\xi)$. One can then consider β as the real part of a complex variable and complete that integral over a semicircle in the complex domain. The resulting integral can be evaluated by calculating the residues, and the expression for W becomes

$$W = -\frac{Y^2}{2} - \alpha_c \frac{Y}{2} + (\alpha_s^2 + \alpha_c^2) \left\{ \sum_{n=1}^\infty (1 - n^2 \sin^2\gamma) n^{-1} \tan(n\gamma) \sin(n\eta) \exp(-n\xi) + \sum_{j=0}^\infty \left[1 - \sin^2\gamma \left(\frac{2j+1}{2}\right)^2 \left(\frac{\pi}{\pi - \gamma}\right)^2\right] \left(\frac{2}{2j+1}\right) \times \frac{\cos\left[\frac{2j+1}{2}\pi\frac{\eta - \gamma}{\pi - \gamma}\right]}{\sin\left[\frac{2j+1}{2}\pi\frac{\gamma}{\pi - \gamma}\right]} \exp\left[-\frac{2j+1}{2}\left(\frac{\pi}{\pi - \gamma}\right)\xi \right] \right\} \tag{12}$$

It is seen that both series in Equation (12) converge rapidly for $\xi = 0$ but rather slowly on the center line. Hence, the two solutions (11) and (12) complement each other, and velocities can be readily calculated anywhere in the domain.

However, it is apparent that the calculation of the average velocity or discharge becomes difficult. Here a different method proves more convenient.

This method is based on the Ritz-Galerkin approach (for details see Kantorovich and Krylov, 1958, p. 272) as applied to the integral:

$$I = \int_Y \int_X [\tfrac{1}{2}(\nabla W)^2 + W] dX dY \tag{13}$$

It is first noted that "of the class of functions W that satisfy condition (4*a*) the one which makes I an extremum also satisfies the governing equation and condition (5*a*)." This is easily shown by adopting the notation and concepts of the calculus of variations. Indeed, the first variation is

$$\delta I = \int\int [\nabla(W) \nabla(\delta W) + \delta W] dX dY = \int (\partial W/\partial n) \delta W ds + \int\int (1 - \nabla^2 W) \delta W dx dy \tag{14}$$

where ds signifies integration only over the free surface.*

It is clear from Equation (14) that if δI vanishes for arbitrary δW, then the multiplier of this term in both integrands should vanish. This proves the quoted statement.

The solution sought can be expressed as

$$W = \sum_{n=1}^N \sum_{m=0}^M A_{mn} X^{2m} Y^n = \sum_{n=1}^N \sum_{m=0}^M A_{mn} \Phi_{mn} \tag{15}$$

In view of the symmetry and condition (4*a*), respectively, terms containing odd powers of X and the terms $X^{2m}Y^0$ are not included. For $(M, N) \to \infty$, the form (15) is a valid representation of W and constitutes a convergent series throughout the domain in question. This is so because the domain does not contain singular points (see

* As W is prescribed on the solid [it satisfies Equation (4*a*)] but not on the free surface, the variation δW vanishes on $Y = 0$ and makes no contribution to the expression for δI, whereas the variation δW on the free surface does contribute. This mixed treatment of the two boundaries differs slightly from those appearing in most texts.

Appendix).* Convergence (Bentwich, 1976) implies that the exact solution can be defined in terms of the doubly infinite set of constants A_{mn} and that an approximate solution of any desired accuracy can be obtained by suitably choosing the upper finite limits M and N. In order to evaluate the coefficients in (15), the results of the preceding paragraph are used. It follows from these that I must be an extremal function of the variables (A_{01}, A_{02}, A_{11}, ...) if the remaining conditions (3*a*) and (5*a*) are to be satisfied. Therefore, it is necessary that

$$\partial I/\partial A_{mn} = 0 \quad m = 0 \ldots\ldots M \qquad n = 1 \ldots\ldots N \tag{16}$$

When Equations (13) and (15) are used, these conditions reduce to

$$\sum_{i=0}^{M} \sum_{j=1}^{N} A_{ij} \int_Y \int_X (\nabla\Phi_{ij} \nabla\Phi_{mn})\, dXdY - \int_Y \int_X \Phi_{mn}\, dXdY = 0 \tag{16a}$$

and this linear set can be easily solved.

Results

It is clear that the accuracy of the modified Ritz-Galerkin scheme improves with larger N and M. However, the most efficient solution will be that which needs a minimum number of terms without producing a significant error. For any given set of polynomials, the maximum velocity (at the North Pole) was found to be a sensitive indicator and will therefore be the only local velocity used here for comparison purposes.

The maximum velocity was first calculated from Equation (11) and is plotted in Figure 3 as a function of the contact angle θ. The integration was performed by using a thirty-two point Gaussian Laguerre quadrature in double precision. To test the accuracy of the evaluation of the integral, different scale factors on β were used, and it was found that the reproducibility deteriorated steadily as θ increased. Thus, at $\theta = 150$ deg. the reproducibility was about 1 in 5 000, while at 160 deg. it was 1 in 500 and at 170 deg. it was 1.5 in 100. It is noted that the plotted values agree with those available from the numerical approach (Kern, 1969) within 1%; hence, the latter are not specifically shown.

Testing the modified Ritz-Galerkin scheme against these results, one finds a surprisingly good agreement when only the first four terms of Equation (15) are used. Since the values of the coefficients will be presented later, only the relative errors of both maximum and average velocities are shown in Table 1. The errors in the average velocities are obtained by comparison with the numerical ones from Kern (1969).

As expected, the four-term expansion becomes less accurate with increasing curvature of the isovelocity lines, that is, for very large as well as very small contact angles. However, it is easy to compute the higher coefficients if improved accuracy is required. The convergence of Equation (15) with increasing number of terms in the expression is illustrated in Table 2. This demonstrates that beyond $\theta = 150$ deg. an unreasonably large number of coefficients would be necessary for high accuracy. On the other hand, such contact angles are unlikely to occur in a physical situation.

* Supplementary material has been deposited as Document No. 02839 with the National Auxiliary Publications Service (NAPS), c/o Microfiche Publications, 440 Park Ave. South, New York, N. Y. 10016 and may be obtained for $3.00 for microfiche or $5.00 for photocopies.

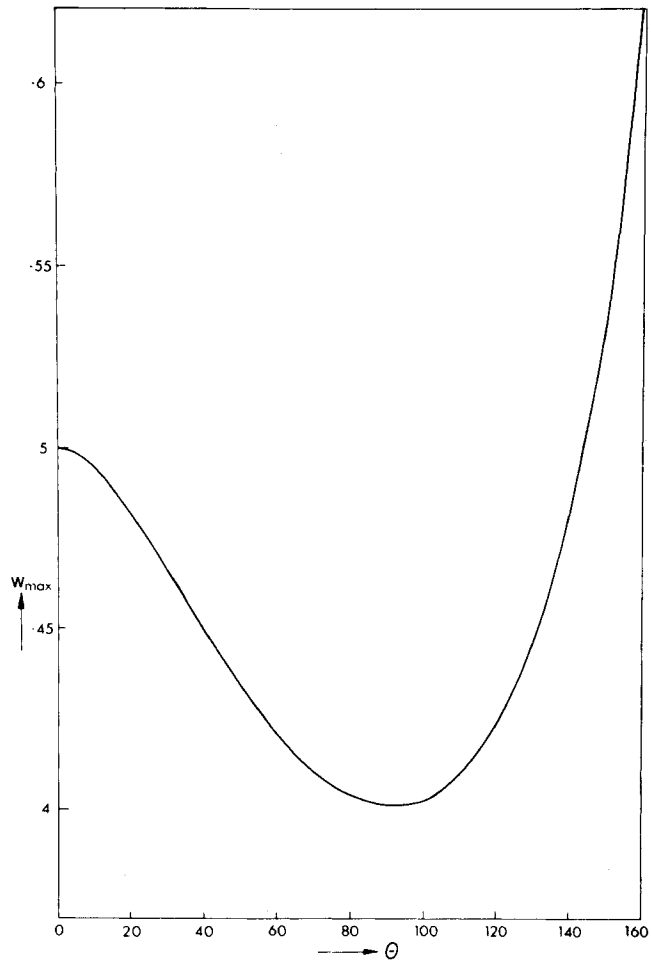

Fig. 3. Maximum surface velocity of a vertical rivulet.

TABLE 1. RELATIVE ERROR OF VERTICAL FLOW ANALYSES

θ	e_{max}	e_{av}
10	—	—
20	0.73	−0.01
30	1.04	−0.05
40	1.03	−0.11
50	0.77	−0.15
60	0.41	−0.15
70	0.07	−0.12
80	−0.07	−0.07
90	0.03	−0.09
100	0.14	−0.44
110	0.29	−0.49
120	0.35	−0.93
130	−0.97	−2.02
140	−3.58	−4.38
150	−8.66	−8.65
160	−17.58	—
170	−33.63	—

$$e_{max} = \frac{W_{max,\,eq.\,(15)} - W_{max,\,eq.\,(11)}}{W_{max,\,eq.\,(11)}} 100\ [\%]$$

$$e_{avg} = \frac{W_{avg,\,eq.\,(15)} - W_{avg,\,numer.}}{W_{avg,\,numer.}} 100\ [\%]$$

FLOW OVER INCLINED PLATE

The important conclusion to be drawn from the previous section is that polynomials of relatively low order are suitable to represent the velocity distribution in a rivulet of constant interfacial curvature. However, this conclusion also applies to flow over an inclined plate along the

Table 2. Convergence of Ritz-Galerkin Solution for Vertical Flow

	$W_{max,eq.(15)}$ Number of coefficients				
θ	4	9	24	40	$W_{max,eq.(11)}$
130	0.4397	0.4408	0.4433	0.4432	0.4440
150	0.4843	0.4935	0.5131	0.5203	0.5302
170	0.5273	0.5585	0.6301	0.6586	0.7945

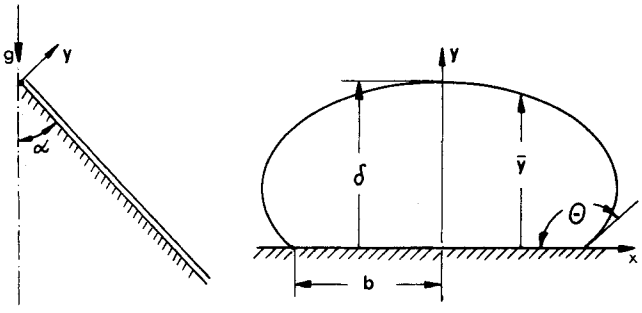

Fig. 4. Coordinate system for rectilinear flow over an inclined plate.

line of largest slope. In this case, the velocity profiles do not change in character, the only additional problem being the more complicated shape of the rivulet. This has been analyzed by many authors so that only a summary will be presented here.

Governing Equations

According to Figure 4, the Navier-Stokes equations take the form

$$\frac{\partial P}{\partial x} = 0 \tag{17}$$

$$\frac{\partial P}{\partial y} = -\rho g \sin\alpha \tag{18}$$

and

$$\frac{\partial^2 w}{\partial x^2} + \frac{\partial^2 w}{\partial y^2} = -\frac{g\cos\alpha}{\nu} \tag{19}$$

The boundary conditions become

$$w(|x| \leq b, y = 0) = 0 \tag{20}$$

and

$$-\frac{d\bar{y}}{dx}\cdot\frac{\partial w}{\partial x} + \frac{\partial w}{\partial y} = 0 \text{ on } y = \bar{y}(x) \tag{21}$$

From Equation (18) and the Laplace-Young equation, one finds the differential equation describing the interface $\bar{y}(x)$:

$$\frac{d^2\bar{y}}{dx^2}\left[1 + \left(\frac{d\bar{y}}{dx}\right)^2\right]^{-3/2} = \frac{\bar{y}}{a^2} - \frac{\delta}{2a^2} - \frac{1-\cos\theta}{\delta} \tag{22}$$

Here we have introduced the capillary constant

$$a = \sqrt{\frac{\sigma}{\rho g \sin\alpha}} \tag{23}$$

which contains all the shape-determining physical properties of the liquid.

It is seen that the solution of Equation (22) is unaffected by Equation (19); that is, the cross section of the rivulet is determined independently of the velocity distribution. However, Equation (21) shows that the converse is not true. Consequently, one has to solve Equation (22) before proceeding to the solution of the flow equation.

For the same reason as before, we nondimensionalize the system with the maximum height of the rivulet; that is

$$X = x/\delta, \quad Y = y/\delta, \quad \bar{Y} = \bar{y}/\delta$$

and

$$W = \frac{w\nu}{\delta^2 g\cos\alpha} \tag{24}$$

It is noted that the capillary constant [Equation (23)] could also serve as a reference length (see Towell and Rothfeld, 1966) and is in fact a more readily available parameter. But in that case, the comparison of velocities at different tilts of the plate becomes rather meaningless; thus we prefer to employ δ rather than a.

The velocity distribution is governed by

$$\frac{\partial^2 W}{\partial X^2} + \frac{\partial^2 W}{\partial Y^2} = -1 \tag{19a}$$

$$W\ (|X| \leq b/\delta, Y = 0) = 0 \tag{20a}$$

and

$$-\frac{\partial\bar{Y}}{\partial X}\cdot\frac{\partial W}{\partial X} + \frac{\partial W}{\partial Y} = 0 \quad \text{on} \quad Y = \bar{Y}(X) \tag{21a}$$

The curved interface is given by

$$\frac{d^2\bar{Y}}{dX^2}\left[1 + \left(\frac{d\bar{Y}}{dX}\right)^2\right]^{-3/2} = \left(\frac{\delta}{a}\right)^2\left(\bar{Y} - \frac{1}{2}\right) - (1-\cos\theta) \tag{22a}$$

with boundary conditions

$$\bar{Y}(X=0) = 1$$

and

$$\frac{d\bar{Y}}{dX}(X=0) = 0 \tag{25}$$

It is known (Goodrich, 1961) that the solution to Equation (22a) can be given only in parametric form. Using the transformations

$$\sin^2\lambda = \frac{1}{1 + \left(\dfrac{1-\cos\theta-\Delta^2/2}{2\Delta}\right)^2} \quad \text{with} \quad \Delta = \delta/a \tag{26}$$

and

$$\frac{d\bar{Y}}{dX} = \tan 2\psi \tag{27}$$

one obtains

$$X = \frac{2}{\Delta\sin\lambda}\left\{E(\psi,\lambda) - E(\pi/2,\lambda) - \left(1 - \frac{\sin^2\lambda}{2}\right)[F(\psi,\lambda) - F(\pi/2,\lambda)]\right\} \tag{28}$$

Here, E and F are the elliptic integrals of the second and first kind, defined by

$$E(\psi,\lambda) = \int_0^\psi (1 - \sin^2\lambda\sin^2\psi)^{1/2} d\psi$$

and

$$F(\psi,\lambda) = \int_0^\psi (1 - \sin^2\lambda\sin^2\psi)^{-1/2} d\psi$$

It also follows, by integrating Equation (22a) once, that

$$\overline{Y} = \frac{1}{2} + \frac{1-\cos\theta}{\Delta^2} - \frac{2}{\Delta\sin\lambda}\left(1 - \sin^2\lambda\sin^2\psi\right)^{-1/2} \tag{27a}$$

Hence, for any combination of parameters Δ and θ, one finds λ from Equation (26), ψ as a function of $\overline{Y}$ from Equation (27*a*), and $X(\psi, \lambda)$ from Equation (28).

Once the flow domain is established, the velocity can be calculated from the Ritz-Galerkin method as given by Equations (15) and (16*a*). However, the general problem is characterized by the additional parameter

$$\Delta = \delta\sqrt{\frac{\rho g\sin\alpha}{\sigma}} \tag{29}$$

Thus, the coefficients of the velocity polynomial now depend on two parameters, Δ and θ. Δ is zero for vertical flow, but we can also specify an upper limit which depends on the contact angle alone. Since

$$\delta_{max} = 2\sin(\theta/2)\sqrt{\frac{\sigma}{\rho g\sin\alpha}} \tag{30}$$

is the maximum height of the rivulet at infinite flow rate (see Rayleigh, 1915), it is clear that

$$\Delta_{max} = 2\sin(\theta/2) \tag{30a}$$

The parameter domain over which velocities have to be calculated is therefore limited to

$$0° \leq \theta \leq 180°$$

and (31)

$$0 \leq \Delta \leq 2\sin(\theta/2)$$

Results

Before we present the numerical results evaluated by the above procedure, it is useful to discuss the general structure of the solution and some limiting values. For this purpose we refer to Figure 5, where the average velocity $\overline{W}$ is plotted qualitatively as a function of the two parameters Δ and θ. For vertical flow ($\Delta = 0$), $\overline{W}$ reaches a minimum value at a contact angle of $\theta \cong 60$ deg. When θ approaches 0 deg., that is, when the rivulet of constant height δ becomes infinitely wide, the limiting value is found by L'Hospital's rule and is

$$\overline{W}(\Delta = 0,\ \theta \to 0°) = 0.229\ldots \tag{32}$$

On the other hand, one can prove that the limiting value for large contact angles is

$$\overline{W}(\Delta = 0,\ \theta \to 180°) = \infty \tag{33}$$

This is true in spite of the fact that the rivulet still maintains a line of contact with the solid surface.

At the maximum value of Δ and any intermediate contact angle, the rivulet again becomes infinitely wide but not in the same way as for the vertical rivulet. Figure 6 illustrates the difference. On the inclined plate, end effects become negligible, and the flow cross section tends to fill the bounding rectangle of finite height [see Equation (30)]. Therefore, the average velocity approaches that of a falling film; that is

$$\overline{W}(\Delta_{max}) = 1/3 \tag{34}$$

On the vertical plate, however, the cross section of the rivulet becomes two-thirds of that of the bounding rectangle when the contact angle approaches zero. Hence, even in the limit the average velocity must be smaller than one-third. The point ($\Delta = 0$, $\theta = 0$ deg.) is thus

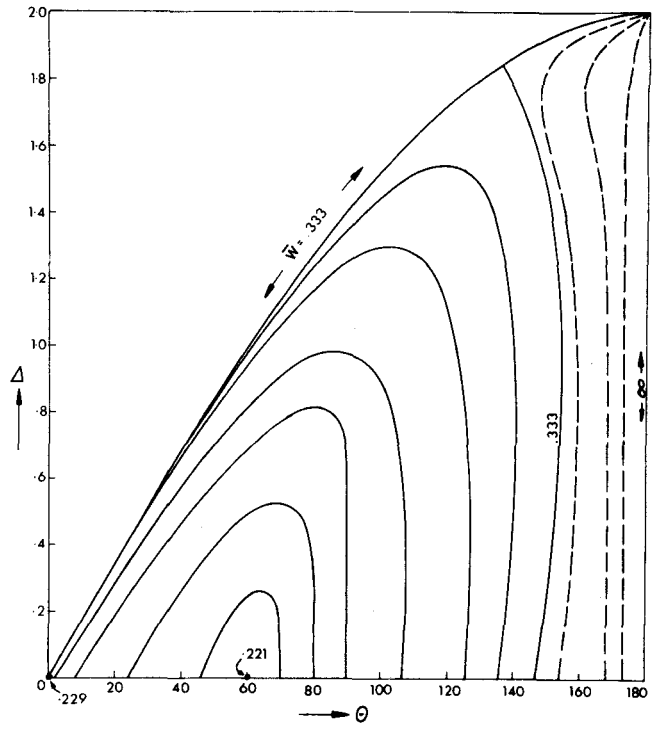

Fig. 5. Qualitative plot of isovelocity lines with limiting values.

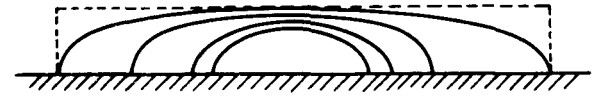

Fig. 6. Approaching infinite wetted width in vertical (top) and inclined flow (bottom).

characterized by a limiting value of $\overline{W}$ which depends on the way we approach the limit. Apparently, the same applies to the point ($\Delta = 2$, $\theta = 180$ deg.). For Δ_{max} and θ fractionally smaller than 180 deg., the wetted width is infinite, and $\overline{W} = 1/3$. Only at the theoretical value of $= 180$ deg. will the wetted width shrink to zero (line contact) so that $\overline{W} = \infty$.

Although these results seem to be of academic interest only, they do supply physical insight into the general flow properties of rivulets and enable one to complete Figure 5 for $0 < \Delta < 2\sin\theta/2$. It is seen that the isovelocity lines are very closely spaced in the important range $\Delta > 0.8\ \Delta_{max}$, so that a different type of graph is required for reading off actual values.

From the numerical calculations it was found that the velocity distribution can again be adequately represented by a second-order polynomial, and the accuracy is satisfactory up to a contact angle of 140 deg. In Table 3 the convergence of the Ritz-Galerkin method is demonstrated by comparing the four with the nine coefficient solution at various values of Δ. Although the table does not show the absolute error for the results, it demonstrates that the trends for $\Delta > 0$ are the same as for $\Delta = 0$. Hence, we conclude that the solution is equally accurate for the inclined and the vertical plate configurations.

Table 3. Convergence of Ritz-Galerkin Solution at Large Contact Angles

		$\theta = 130$ deg.			$\theta = 150$ deg.		
Δ	W	4 coeff.	9 coeff.	9c./4c.	4 coeff.	9 coeff.	9c./4c.
0	max	0.4397	0.4408	1.003	0.4843	0.4935	1.019
	avg	0.2837	0.2877	1.014	0.3350	0.3496	1.044
0.5	max	0.4351	0.4359	1.002	0.4744	0.4809	1.014
	avg	0.2775	0.2809	1.012	0.3226	0.3347	1.038
0.9	max	0.4280	0.4283	1.001	0.4572	0.4608	1.007
	avg	0.2665	0.2690	1.009	0.3006	0.3088	1.027
1.5	max	0.4329	0.4324	0.999	0.4389	0.4394	1.001
	avg	0.2549	0.2558	0.999	0.2692	0.2727	1.013

This is confirmed by further calculations up to twenty-five terms which are not displayed here.

With the solution restricted to four terms, the coefficients can be plotted as a function of Δ and θ so that the velocity at any point of a rivulet is obtainable from four graphs (Figures 7 to 10, available as a microfilm appendix).* In this case, the velocity is expressed as

$$W = A_{01}Y + A_{11}X^2Y + A_{02}Y^2 + A_{12}X^2Y^2 \qquad (35)$$

It should be pointed out that in spite of the separate mathematical treatment, the vertical flow ($\Delta = 0$) now appears as a special case of the inclined flow. This is, of course, expected for purely physical reasons. The maximum velocity at $y = \delta$ ($Y = 1$) is readily evaluated from

$$W_{max} = A_{01} + A_{02} \qquad (35a)$$

However, determination of the average velocity requires integration over the cross-sectional area which, in the general case, cannot be performed analytically. The method of solution employed supplies the volumetric flow rate as a by-product which can be divided by the flow area to obtain the average velocity given in Figure 11. The flow rate or discharge of a rivulet is then calculated from

$$\Omega = \frac{Q \cdot \nu}{\delta^4 g \cos\alpha} = A \cdot \overline{W} \qquad (36)$$

where

$$A = \frac{2}{\Delta^2}\int_{\pi/2}^{\pi/2-\theta} \left[\Delta/2 + (1-\cos\theta)/\Delta - \frac{2}{\sin\lambda} \times (1 - \sin^2\lambda\sin^2\psi)^{1/2} \right] \sin\lambda \frac{1 - 2\sin^2\psi}{(1 - \sin^2\lambda\sin^2\psi)^{1/2}} d\psi \qquad (37)$$

is the cross-sectional area (see Allen and Biggin, 1974). The elliptic integrals can be evaluated from tables. Figure 11, together with Equations (36) and (37), thus supplies all the information required on the integrated properties in a very compact form. The nine coefficient solution for the average velocity at $\theta = 150$ deg. is included in Figure 11 and demonstrates that values larger than one-third are obtained at high contact angles. However, the numerical values cannot be regarded as very accurate because, at this contact angle, the convergence becomes poor, particularly for small values of Δ.

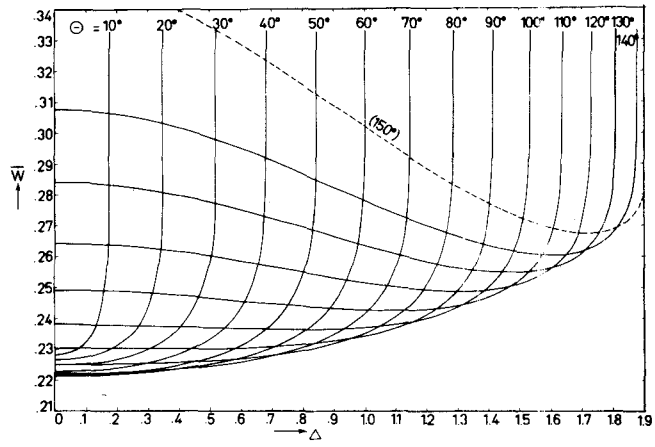

Fig. 11. Average velocity of a rivulet as a function of Δ and θ.

NOTATION

A = dimensionless flow area of rivulet
A_{mn} = Ritz-Galerkin coefficient
a = $\sqrt{\sigma/(\rho g \sin\alpha)}$ = capillary constant, m
b = wetted half width of rivulet, m
D = $R - \delta$ (see Figure 1), m
E, F = elliptic integral of second, first kind
g = acceleration due to gravity, m/s^2
I = integral defined by Equation (13)
i, j, m, n, M, N = integer
P = pressure, N/m^2
Q = volumetric flow rate, m^3/s
R = radius of curvature, m
w = velocity, m/s
$W, \overline{W}$ = dimensionless local, integrated velocity, Equations (7) and (24)
x, y = Cartesian coordinates, m
X, Y = x/δ, y/δ = dimensionless coordinates
$\overline{y}, \overline{Y}$ = interface coordinate, see Figure 4
z = complex variable

Greek Letters

α = tilt of plate from the vertical, degree
α_s, α_c = functions of θ, Equations (4a) and (5a)
$\beta, \bar{\beta}$ = dummy variable
γ = $\pi - \theta$ = function of contact angle
δ = maximum height of rivulet, m
Δ = δ/a = dimensionless maximum height
ζ = complex variable
η = imaginary part of ζ
θ = contact angle, deg.
λ = function of Δ and θ, defined by Equation (26)
ν = kinematic viscosity of liquid, m^2/s
ξ = real part of ζ
ρ = density of liquid, kg/m^3
σ = surface tension of liquid, N/m
ϕ = harmonic function defined by Equation (8)
Φ = function of X and Y defined by Equation (15)
ψ = function of $\overline{Y}$ defined by Equation (27)
Ω = dimensionless flow rate

* See footnote on p. 775.

LITERATURE CITED

Allen, R. F., and C. M. Biggin, "Longitudinal Flow of a Lenticular Liquid Filament down an Inclined Plane," *Phys. Fluids*, **17**, 287 (1974).

Bentwich, M., "Two-Phase Axial Laminar Flow in a Pipe with Naturally Curved Interface," *Chem. Eng. Sci.*, **31**, 71 (1976).

Goodrich, F. C., "The Mathematical Theory of Capillarity," *Proc. Royal Soc.*, **A260**, 481 (1961).

Kantorovich, L. V., and V. I. Krylov, *Approximate Methods of Higher Analysis*, Noordhoff, Groningen (1958).

Kern, J., "Zur Hydrodynamik der Rinnsale," *verfahrenstechnik*, **3**, 425 (1969).

———, "Phenomena and Flow Regimes in Rivulet Flow," submitted to *J. Fluid Mech.* (1975).

Morse, P. M., and H. Feshback, *Methods of Theoretical Physics*, Chapt. IV, McGraw-Hill, New York (1953).

Rayleigh, Lord, "On the Theory of the Capillary Tube," *Proc. Royal Soc.*, **A92**, 184 (1915).

Towell, G. D., and L. B. Rothfeld, "Hydrodynamics of Rivulet Flow," *AIChE J.*, **12**, 972 (1966).

Manuscript received December 30, 1975; revision received May 4 and accepted May 5, 1976.

Electropolarization Chromatography

JOAQUIM F. G. REIS

and

E. N. LIGHTFOOT

Department of Chemical Engineering
University of Wisconsin
Madison, Wisconsin 53706

The utility of electropolarization chromatography for fractionation of native protein mixtures is examined both mathematically and experimentally.

Mathematical prediction based on a simplified but basically realistic model of this process suggests it to be very promising for both analytical and preparative purposes.

This expectation is borne out by tests with well-defined proteins in single ultrafiltration fibers. The major observed departure from model prediction is an unexpectedly sharp increase in retardation at a critical voltage specific to the protein and composition of the carrier electrolyte. This permits sharper separations than previously expected and is thus favorable.

SCOPE

A new process, electropolarization chromatography or EPC, is proposed for the fractionation of native proteins. This process is described qualitatively and in terms of a relatively simple mathematical model which adequately encompasses most of its characteristic behavior. Preliminary experimental results are presented which support the model but also show the possibility of greatly enhanced separation effectiveness under mild process conditions in simple equipment constructed from commercially available materials.

CONCLUSIONS AND SIGNIFICANCE

EPC is inherently superior to such processes as free-flow electrophoresis from the standpoints of resolution, removal of ohmic heat, and suppression of free convection. It can be carried out in very simple equipment at modest voltages, and it offers unusual flexibility, both in choice of operating conditions and scale. Preparative separations appear to be feasible upwards from tens of micrograms without major scale-up problems.

Electrophoresis has been known to be a powerful and flexible means for separating proteins since the pioneering experiments of Tiselius (1937), and it has been used for many years as an analytical tool. It has not yet been very successful on a preparative scale, however, and we have shown (Reis et al., 1974) that this is in part because of excessive convectively induced dispersion (Taylor diffusion). It is in fact clear from our analysis that high resolution will inevitably be accompanied by prohibitive levels of ohmic heating in such processes as free-flow electrophoresis (Hannig, 1964, 1969).

We have accordingly proposed (Lee et al., 1974) as an alternate to free-flow electrophoresis (FFEP) a process we now call electropolarization chromatography (EPC).* In this process, described more completely below, pulses of protein mixtures are added to a carrier solution flowing in a cylindrical duct of convenient cross section. The proteins are then segregated into the neighborhood of the duct wall and hence into slower moving regions of the carrier by the presence of a transverse electric field. The effective axial velocity of each component of the feed is determined by the degree of segregation, and this in turn depends on the electrochemical nature of the protein, in particular its charge density.

We show in a separate mathematical analysis (Reis et al., 1976) that EPC is frequently much superior to FFEP, from the standpoint of potential resolving power, removal of ohmic heat, and control of free convection. We further show that ducts of circular cross section are particularly promising for control of geometry and flow distribution, for ease of heat removal, and for simplicity of manifolding in large systems.

* We have referred to this in the past as electrophoretic single-phase chromatography, and Giddings has used electrophoretic field-flow fractionation. The term EPC, proposed by Peter Rigopulos of Amicon Corporation, is more compact and emphasizes the key role of polarization.